JOURNAL OF MATERIALS SCIENCE 40 (2005) 5359–5363

Electrospun ultra-fine silk fibroin fibers from aqueous solutions

HONG WANG, YAOPENG ZHANG, HUILI SHAO*, XUECHAO HU
State Key Laboratory for modification of Chemical Fibers and Polymer Materials, College of Material Science and Engineering, Donghua University, Shanghai 200051, P. R. China
E-mail: hlshao@dhu.edu.cn

By using electrospinning technique, beaded, cylinder shaped and ribbon like ultra-fine silk fibroin (SF) fibers were obtained from its concentrated aqueous solution under different processing conditions. These fibers had an average diameter of 700 nm and were characterized by scanning electron microscopy (SEM), Wide-angle X-ray diffraction (WAXD) and Raman spectroscopy. It was found that the morphology and the secondary structure of the as-spun SF fibers were strongly influenced by the solution concentration, as well as the processing voltage. By adjusting these technological parameters, β-sheet conformation and silk II crystal structure of the SF fibers can be formed without any post-treatment.

1. Introduction

The dragline filaments produced by orb weaving spiders have been the focus of numerous recent investigations because they are among the strongest known protein fibers [1, 2]. Researchers all over the world are interested in mimicking the native silk fiber and hope to produce artificial silk in vitro for industrial production [3–5]. A number of groups have attempted to spin silk protein fiber from regenerated silk or recombinant spider silk [6–8], using organic or ionic salt solution as solvent or coagulation agent. But the as-spun fibers do not have the same mechanical properties as those of natural silk fibers. As in natural spinning process, however, spider silk and silkworm silk are spun from water to air, so we are more interested in how filaments could be obtained in air from an aqueous solution.

Electrospinning technique has been known since the 1930s. In the past decade, interest in electrospinning process has been arisen [9, 10], because polymer fibers prepared by this technique are able to achieve fiber diameters in the range of nanometer to a few micrometers and have large specific surface area. So the electrospun fibers can be used as filters, membranes, bio-cidal gauzes, scaffolding for tissue build-up and even clothing [11]. There has been a preliminary report of electrospun spider silk nanofibres, using hexafluoro-2-propanol as solvent [12]. And recently So Hyun Kim used formic acid as solvent to electrospin silk nanofibres [13]. But the resultant as-spun silk fiber is only in random coil conformation, which is not stable enough to make the fiber as structural material, and has to be dealt with thermal annealing or methanol treatment to increase its crystallinity.

In this study, spinnable silk fibroin (SF) aqueous solutions with high SF content were first prepared, and then ultra-fine SF fibers were produced from SF aqueous solution by electrospinning process. It is found that SF fibers with β-sheet conformation and silk II crystal structure could be got directly by modifying the electrospinning process.

2. Experimental

2.1. Preparation of SF aqueous solution

Cocoons of *B. mori* silkworms were boiled twice in 0.5%(w/w) $NaHCO_3$ solution for 30 min each, then rinsed thoroughly with distilled water and allowed to air dry at room temperature. The degummed silk was dissolved in 9.3 M LiBr aqueous solution at room temperature to a concentration of 10 wt%. It was then diluted with three times of distilled water and dialysed against distilled water for three days to obtain SF aqueous solution with concentration of about 2%. Highly concentrated SF aqueous solutions with desired concentrations were prepared with procedure developed in this lab.

2.2. Production of electrospun fibers

SF aqueous solution was placed into a plastic capillary, which was attached with a metal needle. A pump injector was connected to the syringe to control the flow rate of SF aqueous solution. A flat piece of aluminium foil, placed 12 cm from the needle, was used to collect the electrospun material. A high voltage of 10–40 kV was applied to the receiving aluminium foil.

*Author to whom all correspondence should be addressed.
0022-2461
DOI: 10.1007/s10853-005-4332-2

TABLE I Process parameters of electrospun SF fiber samples

Sample number	L1	H1	L2	H2	L3	H3
Concentration (wt%)	17	17	28	28	39	39
Voltage (kV)	20	40	20	40	20	40
Diameter (nm)	–	–	400–800	400–1000	100–500	400–1000

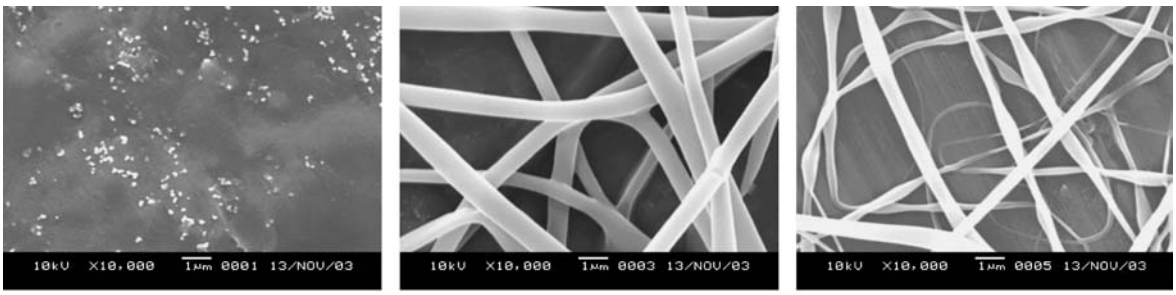

Figure 1 SEM photographs of electrospun SF fibers: (a) sample L1, (b) sample L2, (c) sample L3.

The electrospinning process was carried out at room temperature.

The process parameters of all the electrospun SF fiber samples of this paper were summarized in Table I.

2.3. Characterization

The morphology of the electrospun SF fiber was observed with a scanning electron microscope (SEM, JSM-5600LV) at 10 kV. All samples were sputtered with gold.

Wide-angle X-ray diffraction (WAXD) patterns were measured by a reflection method and recorded on a Rigaku D/Max-BR diffractometer, using Cu-K_α radiation (λ=1.54 Å) in the 2θ range of 5–40° at 40 kV.

Raman spectra were obtained using a Lab RAM-1B microscopy Raman microscope. The 632.8 nm red line of a He-Ne laser was focused on the sample.

Rheological measurements were performed on a HAKKE RS150 rheometer using a 35/1° cone and plate. The shear rate was linearly increased without oscillation from 0.1 to 1000 s^{-1}. Temperature was controlled at 25±0.1°.

3. Results

3.1. The effects of concentration on the morphology of fibers

Fig. 1 showed SEM photographs of silk fibers prepared from SF aqueous solutions with concentrations of 17, 28 and 39% under same spinning conditions. It could be found that the morphology of the SF fibers was strongly affected by the concentration of solution. When the solution concentration was as low as 17 wt%, there were only small droplets on the aluminium foil. When the concentration was as high as 28 wt%, the as-spun SF fibers exhibited a circular cross-section with a smooth surface, and had diameters ranged from 400 to 800 nm. When the concentration was as high as 39 wt%, however, the SF fibers became uneven and ribbon-shaped, and there was also a big variation of fiber diameter ranged from 100 to 600 nm. In any case, all the fibers were much thinner than raw SF fibers (*B. mori* = 10–20 μm).

To further investigate the influence of the solution concentration on the morphology of electrospun SF fibers, the rheological behavior of the SF aqueous solutions was studied. Fig. 2 was the flow curves for SF aqueous solutions with different concentrations. There was a rapid initial shear thinning at low shear rates ($\leq$10 s^{-1}) for SF aqueous solutions with concentrations of 17 and 28%, after which their viscosity remained approximately constant up to 40 mPa·s and 250 mPas respectively. However, the shape of rheological curve of SF aqueous solution with concentration of 39% was very different from those of the above two SF solutions. Its viscosity was almost constant up to 3000 mPa·s when the shear rate was low than 1000 s^{-1}, after which the shear thinning phenomenon became more visible.

When the concentration of SF aqueous solution was 17 wt%, SF macromolecules were in random-coil conformation without entanglement between them. As a result, the viscosity of the solution after shear thinning was only about 40 mPa·s. During electrospinning process, the solution was almost deposited from

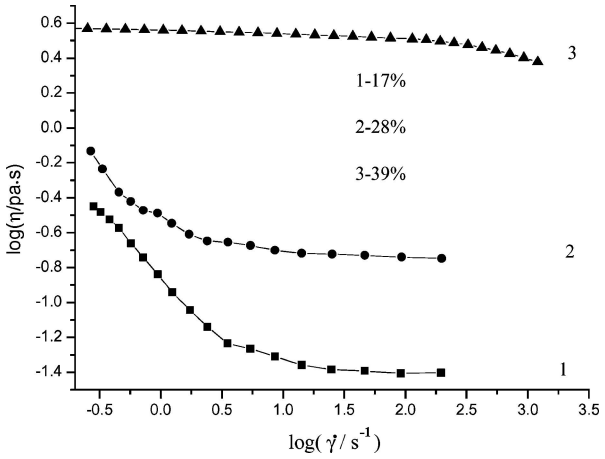

Figure 2 Flow curves for SF aqueous solutions with different concentration.

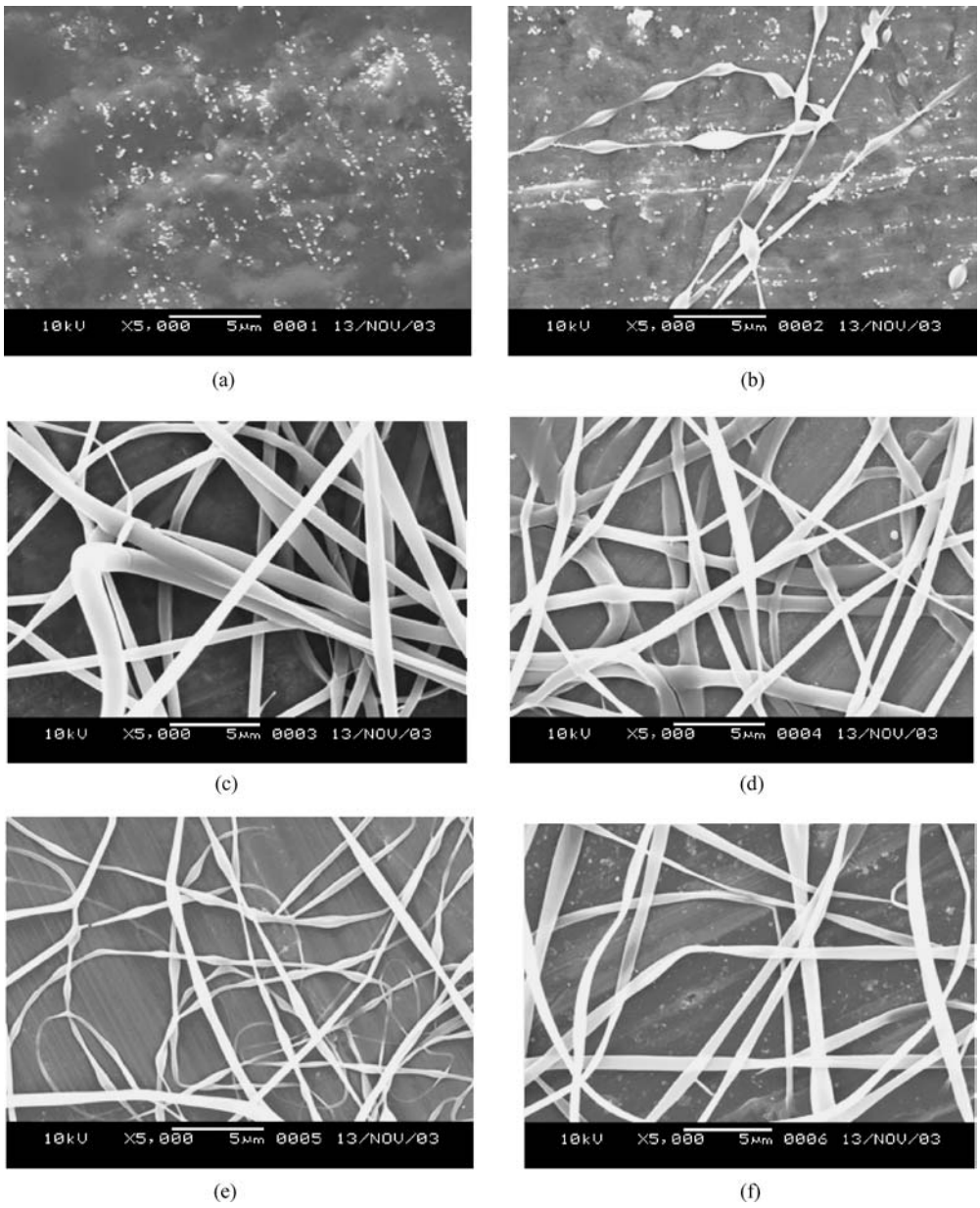

Figure 3 SEM photographs of electrospun SF fibers: (a) sample L1, (b) sample H1, (c) sample L2, (d) sample H2, (e) sample L3 (f) sample H3.

spinneret as individual droplets on the aluminium foil. The viscosity of SF solution increases with increasing SF concentration. When the concentration of the SF solution was as high as 28 wt%, the viscosity of the SF solution after shear thinning reached about 250 mPa·s. There were evidently sufficient molecular chain entanglements in the solution to prevent the breakup of the electrically driven jet and to allow the electrostatic stresses to further elongate the jet and draw it into fibers [14]. But when the concentration of the SF solution was as high as 39%, the viscosity of the SF solution was as high as 3000 mPa·s to make the solution instable and inhomogeneous, so the electrospun SF fibers became uneven and ribbon-shaped. Another reason for the ribbon shape is that the viscosity of the solution is too high for water to evaporate easily from the fibers surface, so fibers have to solidify on the aluminium foil and becomes flat. On the whole, in certain range of solution concentration, when the viscosity of the solution is appropriate, electrospun SF fiber with circular cross-section and smooth surface can be achieved. While in lower range of concentration, droplets or beaded fibers occurred, and in upper range of concentration, the SF fibers became uneven and flat.

3.2. The effects of voltage on the morphology of fibers

The effects of the voltage applied during electrospinning on the SF fibers, which were produced from SF solutions with different concentrations, were also investigated, and the SEM photos were shown in Fig. 3. For the solution with low concentration of 17 wt%, there was little entanglement between SF macromolecules. The polymer jet only formed droplet at low voltage, because the electrostatic force could not overcome the surface tension [15] (Fig. 3a). With higher voltage applied, the strong electrostatic force overcame the surface tension, however, the jet still had the tendency to contract into droplet. As a result, some beaded fibers were formed, although the viscosity of the SF solution was very low (Fig. 3b). When the concentration of the

solution was 28 wt%, it formed round cross-sectional electrospun SF fibers with a smooth surface at low voltage (Fig. 3c). As the intensity of the electric field was increased, the spinning rate increased quickly, so water in the jet had no time to vaporize completely from the fiber surface before it arrived the foil, and the fiber became ribbon-like consequently [16] (Fig. 3d). But when the concentration of the SF solution was as high as 39 wt%, the viscosity of the solution became very high, making the spinning process unstable and fiber with irregular morphology was formed (Fig. 3e). With the increase of voltage, the high electrostatic power made the concentrated SF aqueous solution flow more easily, so the resultant fibers became more regular by comparison with sample L3 (Fig. 3f). On the same time, because the viscosity of 39 wt% SF solution was very high, it was not easy for water in the jet to diffuse and vaporize from the fiber surface before it arrived the foil, the fiber becomes ribbon-like again.

In conclusion, the solution concentration and spinning voltage have some influence on SF fiber morphology. The conditions for producing beadless round cross-sectional silk fibers electrospun from aqueous SF solutions were found to be as follows: SF concentration 28 wt%, voltage 2 kV, working distance 12 cm.

3.3. Crystal structure of electrospun SF fibers

It was reported that SF exhibits at least three conformations or crystalline: random coil, silk I and silk II. Silk II is the most stable structure and endows silk fiber with excellent mechanical properties [17]. Silk II is commonly thought to be constituted by β-sheets [18]. Through WAXD measurement, some information about the crystalline structure and conformation of SF fibers can be obtained from its crystal structure transition. The principal X-ray diffraction peaks of silk II are 9.7×10^{-10} m ($2\theta = 9.1°$, with CuK$_\alpha$), 4.69×10^{-10} m ($2\theta = 18.6°$), 4.3×10^{-10} m ($2\theta = 20.7°$) and 3.67×10^{-10} m ($2\theta = 24.3°$) [19].

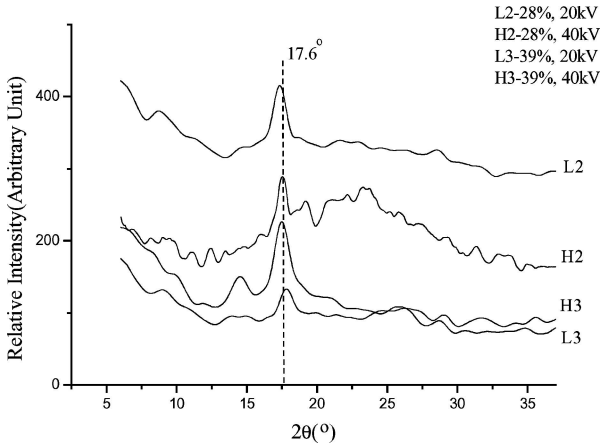

Figure 4 WAXD curves for electrospun SF fibers.

Fig. 4 shows the WAXD intensity curves for electrospun SF fibers formed under different conditions. There is a diffraction peak at 2θ of about 17.6° in all samples, and the peak is shifted to larger angle close to 18.6° with the increase of voltage as well as solution concentration, corresponding to silk II crystal structure [20]. This means that SF macromolecules undergo a conformation transition during the electrospinning process. Silk II structure appears in the electrospun SF Fibers after electrospinning process, and the SF fibers have β-sheet conformation correspondingly.

3.4. Secondary structure of electrospun SF fibers

Raman spectroscopy under a microscope is a powerful tool to investigate the secondary structure of proteins and has already given important insights into the structure of native silk filaments of both spiders and silkworms [21]. All the secondary structures of proteins (α helix, β-sheet, and random coil structures)

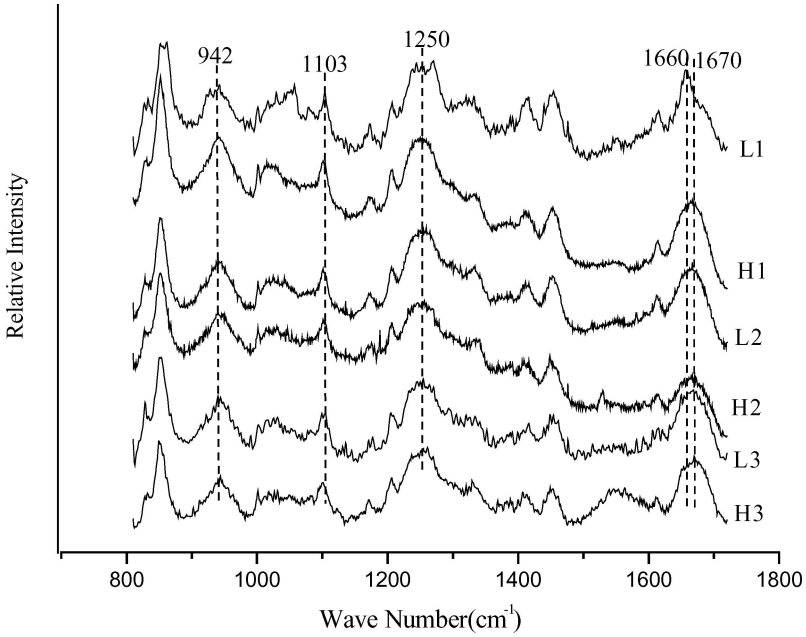

Figure 5 Raman spectra of electrospun SF fibers.

have characteristic band at amide I(1680–1640 cm^{-1}) and III(1270–1220 cm^{-1}) [5, 22]. At amide I, α helix appears at lower wave number and β-sheet appears at higher wave number. But at amide III, β-sheet appears at lower wave number and α helix appears at higher wave number. Their characteristic bands in the Raman spectrum are as followed [5]: 1245 $\pm$ 5 cm^{-1}, 1665 $\pm$ 5 cm^{-1} (random coil); 1270–1300 cm^{-1}, 1654 $\pm$ 5 cm^{-1} (α helix); 1225–1245 cm^{-1}, 1670 $\pm$ 5 cm^{-1} (β-sheet). The peaks at 942 and 1105 cm^{-1} are also sensitive to α helix, and the peak at 1085 cm^{-1} is sensitive to β-sheet too. The Raman spectrum of our electrospun SF fibers was shown in Fig. 5. All samples had bands at about 942 and 1103 cm^{-1}, which meant that α helical conformation existed in all samples. For sample L1, there was a distinct band at about 1656 cm^{-1} (characteristic band of α helix), the amide III band split into 1242 cm^{-1} (characteristic band of random coil) and 1267 cm^{-1} (characteristic band of α helix). It appeared two bands around 930 cm^{-1} (characteristic band of random coil) and 940 cm^{-1} (characteristic band of α helix). These all suggested that SF was mainly in α helix conformation with some random coil. For sample H1, the amide I band appeared at 1670 cm^{-1} (characteristic band of β-sheet), amide III band appeared at about 1250 cm^{-1} (characteristic band of α helix), and the bands around 940 cm^{-1} were merged into a single one. These all suggested that the random coil conformation disappeared. For sample L2, there was a distinctive peak at 1670 cm^{-1} in amide I. And a sensitive band of 1085 cm^{-1} appeared in sample L3 and H3. All in one word, it was found that the random coil conformation disappeared and β-sheet appeared gradually in the electrospun SF fibers with the increase of voltage and concentration of SF solution. Thus the Raman spectral result in Fig 5 is consistent with the WAXD result in Fig. 4.

4. Conclusions

By using electrospinning technique, beaded, round cross-sectional and ribbon shaped ultra-fine SF fibers were obtained from its concentrated aqueous solution under different spinning conditions. These fibers had an average diameter of 700 nm ranged from 100 to 1000 nm. The conditions for preparing beadless circular cross-sectional electrospun SF fibers were found to be as follows: SF concentration 28 wt%, voltage 2 kV, working distance 12 cm. From investigation of WAXD and Raman spectroscopy, it is found that this kind of SF fiber has silk II structure and in α helix and β sheet conformation. It could be expected to get more β-sheet conformation in SF fiber by improving the spinning conditions and solution concentration.

Acknowledgments

The authors thank for the financial support by Hi-Tech Research and Development Program of China (863), No.2002AA336060.

References

1. D. P. KNIGHT and Z. SHAO, *Nature* **418** (2000) 741.
2. C. VINEY, *J. Text. Inst.* **3** (2000) 2.
3. X. CHEN, Z. SHAO, D. P. KNIGHT and F. VOLLRATH, *Acta. Chimica. Sinica.* **l60**(12) (2002) 2203.
4. J. HYOUNG-JOON and D. L. KAPLIN, *Nature* **428** (2003) 1057.
5. C. RIEKET and F. VOLLRATH, *Int. J. Biol. Macromol.* **29** (2001) 203.
6. X. CHEN, D. P. KNIGHT, Z. SHAO and F. VOLLRATH, *Biochem.* **141** (2002) 14944.
7. Z. SHAO, F. VOLLRATH, YONG YANG and H. C. THOGERSEN, *Macromolecules* **36** (2003) 1157.
8. S. ARCIDIACONO, C. M. MELLO, B. MICHELLE, W. ELIZABETH, J. W. SPARES, A. ALFRED, Z. DAVID, L. THOMAS and C. SUASAN, *Macromolecules* **35** (2002) 1262.
9. J. ZENG, X. S. CHEN and X. Y. XUE, *J. Appl. Polym. Sci.* **89** (2003) 1085.
10. R. V. N. KRISHNAPPA, K. DESAI and C. M. SUNG, *J. Mater. Sci.* **38** (2003) 2375.
11. X. H. ZHONG. S. F. RAN and D. F. FANG, *Polymer* **44** (2003) 4959.
12. S. ZARKOOB, D. H. RENEKER and R. K. EBY, *Polym. Preprints* **39** (1998) 244.
13. S. H. KIM, Y. S. NAM, T. S. LEE and W. H. PARK, *Polym. J.* **35** (2003) 185.
14. H. FONG, I. CHUN and D. H. RENKER, *Polymer* **40** (1999) 4585.
15. W. K. SON, J. H. YOUK, T. S. LEE and W. H. PARK, *Polymer* **45** (2004) 2959.
16. A. FRENOT, S. IOANNIS and CHRONAKIS, *Curr. Opin. Colloid In.* **8** (2003) 64.
17. M. Z. LI, Z. Y. WU, N. MINOURA and H. J. YAN, *J. Donghua University (Eng. Ed.)* **19**(3) (2002) 1.
18. M. G. KEVIN and K. DAVID, in "Protein-Based Materials" (K. McGrath and D. Kaplan, Boston, 1997) p. 103.
19. T. ASAKURA, A. KUZUHARA, R. TABETA and H. SAITO, *Macromolecules* **18** (1984) 1841.
20. T. Y. YU and G. X. LI, *ACTA Polym. SIN.* **4** (1993) 415.
21. S. D. ZHENG, G. X. LI and W. H. YAO, *Appl. Spectrosc.* **43**(7) (1989) 1269.
22. D. B. GILLESPIE, C. VINEY and P. YAGER, in "Silk polymers: Materials Science and Biotechnology" (Washington DC: American Chemical Society, 1994) p. 352.

Received 10 July 2004
and accepted 14 February 2005